Giant Mesozoic Coelacanths (Osteichthyes, Actinistia) Reveal High Body Size Disparity Decoupled From Taxic Diversity

Lionel Cavin (lionel.cavin@ville-ge.ch)
Natural History Museum of Geneva
André Piuz
Natural History Museum of Geneva
Christophe Ferrante
Natural History Museum of Geneva
Guillaume Guinot
Institut des Sciences de l'Evolution de Montpellier

Research Article

Keywords: morphological evolution, taxic diversification, Genomic and physiological characteristics

Posted Date: March 2nd, 2021

DOI: https://doi.org/10.21203/rs.3.rs-245480/v1

Giant Mesozoic coelacanths (Osteichthyes, Actinistia) reveal high body size disparity decoupled from taxic diversity

Lionel Cavin[1*], André Piuz[1], Christophe Ferrante[1,2] & Guillaume Guinot[3]

[1] Department of Geology and Palaeontology, Natural History Museum of Geneva, Geneva, Switzerland

[2] Department of Earth Sciences, University of Geneva, Rue des Maraîchais 13, 1205 Genève, Switzerland

[3] Institut des Sciences de l'Evolution de Montpellier (Université de Montpellier, CNRS, IRD, EPHE), Montpellier, France

* Corresponding author

Email: lionel.cavin@ville-ge.ch

Abstract

The positive correlation between speciation rates and morphological evolution expressed by body size is a macroevolutionary trait of vertebrates. Although taxic diversification and morphological evolution are slow in coelacanths, their fossil record indicates that large and small species coexisted, which calls into question the link between morphological and body size disparities. Here, we describe and reassess fossils of giant coelacanths. Two genera reached up to 5 meters long, placing them among the ten largest bony fish that ever lived. The disparity in body size adjusted to taxic diversity is much greater in coelacanths than in ray-finned fishes, and is decoupled from a high rate of speciation or a high rate of morphological evolution. Genomic and physiological characteristics of the extant *Latimeria* may reflect how the extinct relatives grew to such a large size. These characteristics highlight new evolutionary traits specific to these "living fossils".

Introduction

Body size is often used as a proxy for analyzing morphological disparity, and this element is one of the main evolutionary traits discussed by biologists and paleontologists in order to decipher macroevolutionary processes. For example, a general increase in body size over time within animal lineages was one of the earliest nomological law in biology raised by Cope and Depéret[1], and has subsequently been regularly confirmed for various clades (e.g.[2]). Recent studies have shown positive correlations between speciation rates and morphological evolution expressed in body size (e.g.[3,4]). However, body size is only one of the many traits that characterize morphological disparity, which can be measured by many other parameters

(e.g.[5]), and the assumption that body size disparity directly reflects morphological disparity can be questioned.

Coelacanths form a depauperate group of sarcopterygian fish with only one genus today but with a long evolutionary history. These fish are nicknamed "living fossils" because they possess characteristics used by Darwin to characterize this ill-defined concept, in particular "new forms ... have been more slowly formed"[6] (Darwin, however, did not cite the coelacanths, known only from fossils at that time, as examples of "living fossils"). Indeed, the clade exhibits low taxic diversity since its origins in the Devonian (ca 420 Mya) with approximately 63 genera in total. Only three weak successive peaks of higher taxic diversity are recorded in the Upper Devonian, in the Late Carboniferous and in the Middle Triassic (e.g.[7]). Huxley (1866)[8] has already noticed the low anatomical disparity of coelacanths throughout their history, and this observation has been confirmed by most subsequent studies[9,10,11,12,13,14,15]. This monotonic rate of evolution is interrupted by at least three episodes of increased morphological disparity, with forms presenting a different Bauplan, roughly contemporary with peaks of taxic diversity. The rate of genetic evolution within the coelacanth lineage is found by most studies to be slower than that of other vertebrate lineages in the mitochondrial genome[16,17,18] as well as in the nuclear genome[19], at least for the protein-coding genes[20,11].

Extinct giant coelacanths, i.e. fish several meters long, have long been described among the mawsoniids with *Mawsonia gigas* by Woodward in 1907[22], from the Early Cretaceous of Brazil, then with *Axelrodichthys lavocati* from the ‘mid’ Cretaceous of North Africa (e.g.[23,24]), with *Trachymetopon* sp.[25] from the Middle Jurassic of Europe, but also among the latimeriids with *Megalocoelacanthus* from the Late Cretaceous of North America [26,27]. The fossil record of coelacanths reveals a relative abundance of large-sized species, but this

feature has never been regarded as an evolutionary trait that characterizes the clade, except by Wenz[23], who pointed out a general trend towards large size within several Mesozoic lineages.

Here we describe new fossil remains from the Middle Jurassic of Normandy, France, representing one of the largest known coelacanths ever reported. The specimen, a piece of a braincase, was found in the same deposits as fragmentary fossils interpreted as embryos or newborns of the same species. We further reassess the Mesozoic fossil record of giant coelacanths and provide a large-scale comparison of body size disparity versus taxic diversity between coelacanths (Actinistia) and ray-finned fishes (Actinopterygii) over the Devonian - Paleocene time interval. We show that the per capita/taxon coefficient of body size variance is higher than that of ray-fin fishes. This result calls into question the positive correlation between speciation rates and body size found in most vertebrate lineages, and more generally questions the use of body size as a valid proxy for anatomical disparity.

Institutional abbreviations

DGM, Divisão de Geológia e Mineralogia, Departamento Nacional da Produção, Mineral, Rio de Janeiro; **CCK**,Columbus (Georgia) College; **MHNG GEPI**, Natural history Museum of Geneva, Switzerland (palaeontological collection); **MPV**, Paléospace, palaeontological museum of Villers-sur-Mer; **UFMA**, Coleção Paleontológica da Universidade Federal do Maranhão; **UMI**, University Moulay Ismail of Meknès, Morocco.

Results

New material, geographical and stratigraphic provenances

A large, almost complete, basiphenoid of a coelacanth with the posterior end of the parasphenoid sutured ventrally and the posterior part of the posterior parietals sutured dorsally (MHNG GEPI 5778) has been spotted in the paleontological collections of the Geneva Natural History Museum, Switzerland. No labels nor information were associated with this specimen. A search in the museum's archives to trace the origin of the specimen was unsuccessful. The fossil was mechanically and chemically prepared, with 10% diluted HCl. The sediment recovered during the preparation of specimen was prepared by acetolysis in order to extract microfossils. The material recovered includes vertebrae and teeth of small fish, diverse micro-gastropods, as well as micro-bivalves, crinoids (roveacrinids), bryozoans, and foraminifera. The diversity of foraminifera is relatively low, consisting of moderately preserved epistominids and lenticulinids. The recognized species (Fig. 1) are *Epistomina* ex. gr. *mosquensis* Uhlig 1883, *Epistomina* ex. gr. *uhligi* Mjatliuk 1953, *Lenticulina quenstedti* (Gümbel 1862), *L. muensteri* (Roemer 1839), *L. subalata* (Reuss 1854) and *Planularia beierana* (Gümbel 1862). These taxa have only moderate biostratigraphic value, being mainly widespread in the Upper Jurassic (Supplementary Figure S1). The presence of a modern barnacle shell on the fossil (Supplementary Figure S2A), an evidence of its discovery from a locality situated near the seashore, associated to the general type of preservation of the specimen and to the presence of nodosariids and epistominids associated with vertebrate fossils are strong indications that this specimen probably comes from the late Callovian "Marnes de Dives", probably from the well-exposed cliffs of the "Vaches Noires", Villers-sur-Mer, Normandy, France [28]. This facies generally contains an abundance of encrusted gryphaeid oysters as seen on the skull of the coelacanth bearing several of these shells on one of its sides (Supplementary Video, Fig. 2, Supplementary Figure 2B). In addition to these shells, the matrix of the specimen bore the imprint of an ammonite, reminiscent of *Heticoceras* (Christian Meister, Antoine Pictet, personal communication 2014) and a

gastropod shell (Supplementary Figure S2C, D). The "Marnes de Dives" are the equivalent of the lower part of the "Oxford Clay" of Dorset, UK. It is assumed that the specimen reached the Geneva Natural History Museum near its inception in 1820 (it was then called the Academic Museum), along with other fossil vertebrates from Normandy, France.

Recently, two small basisphenoids of coelacanths (MPV 2020.1.13) were discovered by Elisabeth and Gérard Pénnetier from a Callovian strata of the foreshore at the foot of the cliffs of the "Vaches Noires", Villers-sur-Mer, Normandy, France, and therefore come from the same formation as the large basisphenoid.

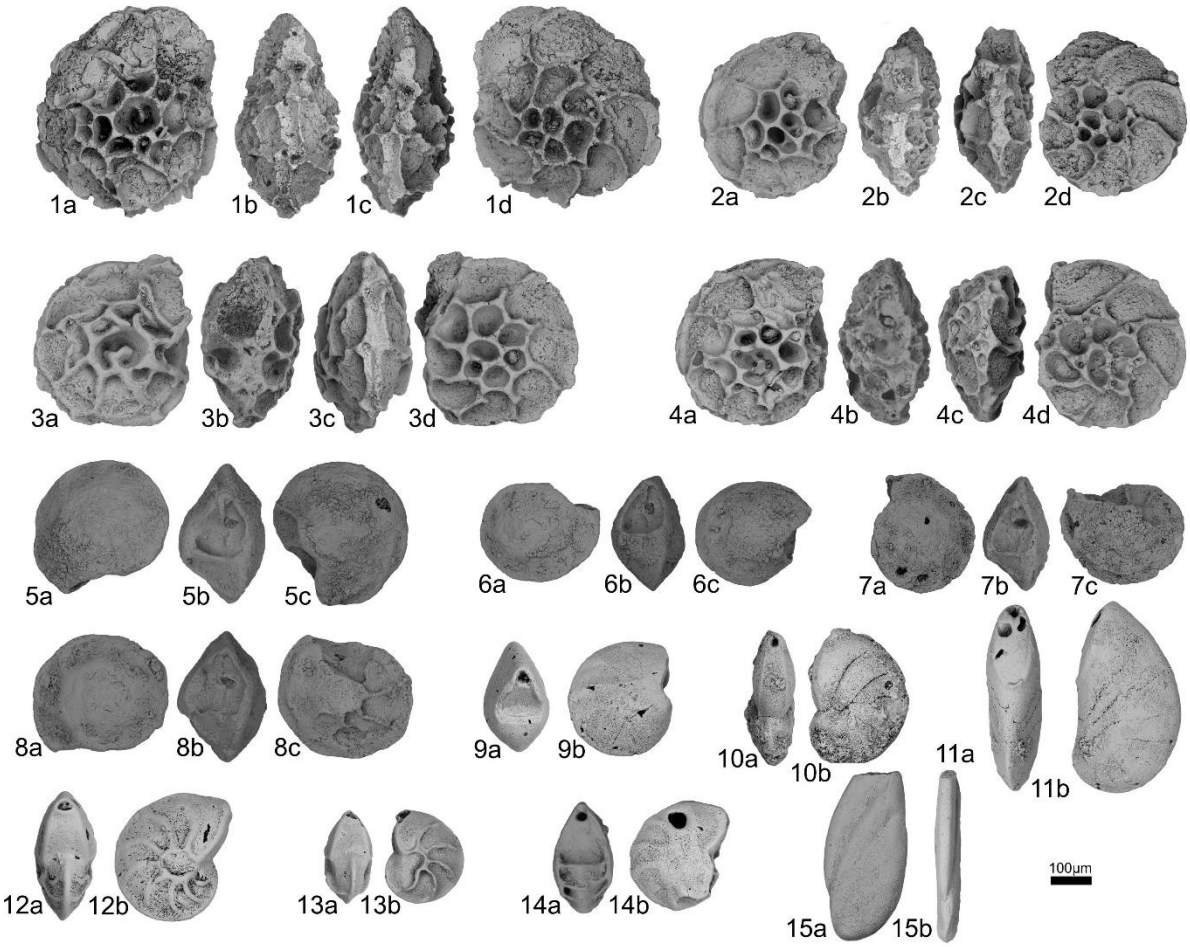

Figure 1

Foraminifera found in the matrix containing the fragment of the coelacanth skull (MHNG GEPI V5778). 1-4, *Epistomina* ex. gr. *mosquensis* Uhlig 1883, umbilical, apertural, carinal and spiral views; 5-8, *Epistomina* ex. gr. *uhligi* Mjatliuk 1953, spiral, apertural and umbilical views; 9-11, *Lenticulina muensteri* (Roemer 1839), apertural and lateral views; 12-13, *Lenticulina quenstedti* (Gümbel 1862), apertural and lateral views; 14, *Lenticulina subalata* (Reuss 1854), apertural and lateral views; 15, *Planularia beierana* (Gümbel 1862), lateral and apertural views.

Morphological description and comparisons

The large specimen (MHNG GEPI V5778) consists of a complete basisphenoid, in connection dorsally with the posterior part of the skull roof and ventrally with a fragment of the parasphenoid (Fig. 2). The processus connectens are well developed, slightly curved in lateral view and extend ventrally to the level of the parasphenoid. The dorsum sellae is proportionally short and forms anteriorly a shallow wall that constricts ventrally the entrance to the cranial cavity. On the posterior side of the bone, the well-developed and closely spaced sphenoid condyles are separated from each other by a marked notch and from the paired processus connectens by shallow depressions. The opening of the cranial cavity is much deeper than wide, with its dorsal part slightly wider than its ventral part. The antotic processes protrude laterally and suture dorsally to the ventral processes of the posterior parietal. The surfaces of contact between both processes are large and oval. The suprapterygoid fossa is well marked but shallow. Anteriorly, a large foramen opens oriented frontwards. Within the ossification, just behind the opening, the canal is divided by a thin horizontal lamina, which separates a larger ventral canal from a smaller dorsal one (Fig. 2D). Based on the paths of the nerves in *Latimeria*[11], the small dorsal canal may have accommodated the superficial ophthalmic nerve and the ventral canal the trochlear nerve (IV). In *Latimeria*, but also in most

post-Paleozoic taxa in which this part of the braincase is preserved, such as *Megalocoelacanthus*[27] and *Trachymetopon*[29], the nerves exit the cranial cavity in the interorbital cartilage. In the Devonian genera *Diplocercides* and *Euporosteus*[11], the nerves exit through bone-enclosed foramens. We interpret the occurrence of this large foramen in MHNG GEPI V5778 as a consequence of the large size of the individual and its high degree of ossification rather than affinities with Paleozoic forms. Ventral to the large foramen, and present on both sides of the basisphenoid, opens the small oculomotor foramen. The angle between the posteroventral surface of the basisphenoid and the ventral surface of the parasphenoid is approximately 135°. The basipterygoid and suprapterygoid processes are absent.

The posterior parts of both posterior parietals are still sutured to the basisphenoid. The portion exposed to the surface of the skull roof, ornamented with faint anastomosed longitudinal ridges, is divided in two parts: a horizontal median part and an inclined lateral part on each side, forming an angle of approximately 120° with the horizontal part in posterior view. At the posterolateral edge of the inclined part of the postparietal opens a large foramen for the entry of supraorbital sensory canal. Along the lateral margin of the left preserved part of the posterior parietal open four small pores for the supraorbital sensory canal. The descending process of the posterior parietal extends ventroposteriorly from the inclined part of the bone. Posteriorly opens a large rounded foramen for the superficial ophthalmic nerve.

Although no diagnostic characters of *Trachymetopon liassicum* identified by Dutel et al.[29] are observable on the specimen, except its large size, several features allow referring this material to this species: in lateral view the basisphenoid is triangular in shape with a curved lateral margin and a short dorsum sellae; the antotic process and processus connectens are well developed, the latter reaching the parasphenoid; the opening for the cranial cavity is deeper than wide and its outline is quadrangular (slightly wider dorsally than ventrally in our

specimen); a marked notch separates the short and divergent sphenoid condyles; and the angle between the posteroventral surface of the basisphenoid and the ventral surface of the parasphenoid is approximately 135°. The only significant difference between the material of *T. liassicum* described by Dutel et al.[29] and ours is that the anterior margin of the intracranial joint is straight in the former, while it has two marked notches in the latter. We notice, however, that the material of *T. liassicum* from Holzmaden figured by Hennig[30] and Dutel et al.[29] is apparently not very well preserved in this area. Consequently, MHNG GEPI V5778 is referred here to *Trachymetopon* sp. The general morphology of the specimen is also very similar to those of other mawsoniids, in particular *Mawsonia* and *Axelrodichthys*. Estimation of the total length of this individual based on proportions of the type specimen of *T. liassicus* is 5 meters (see below).

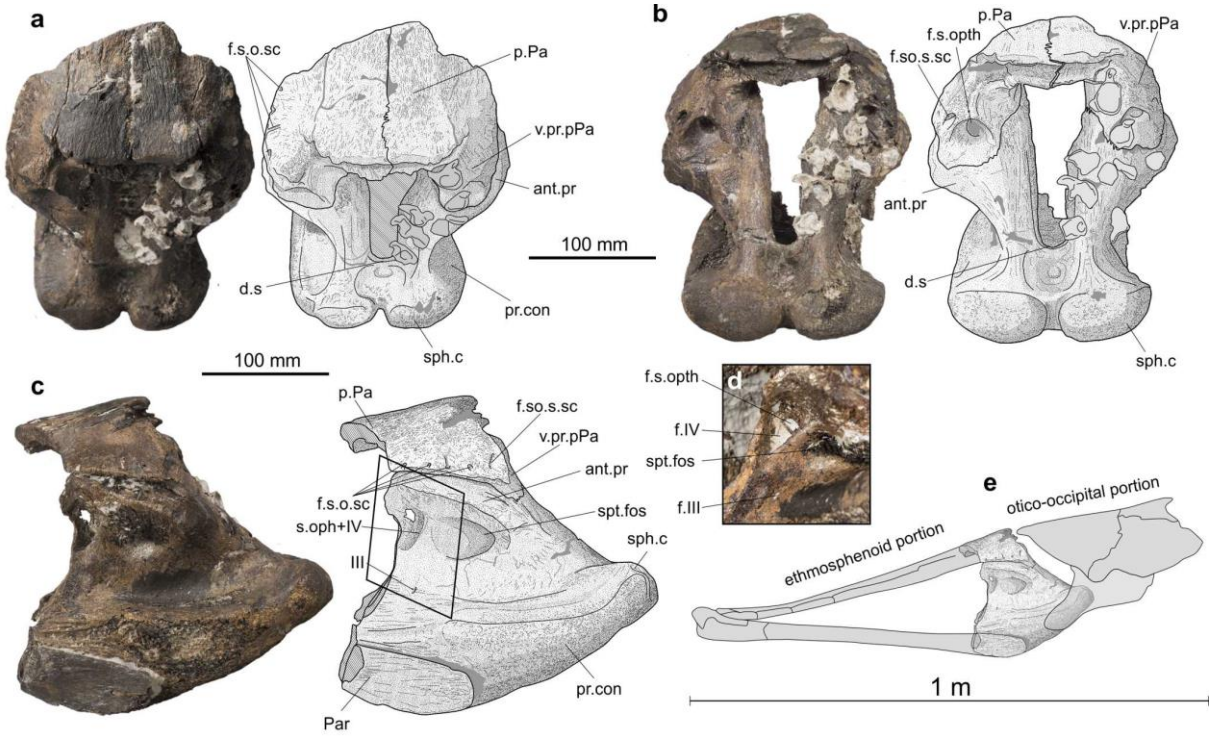

Figure 2

MHNG GEPI V5778. *Trachymetopon* sp. Basisphenoid with fragments of the posterior parietals and parasphenoid. Dorsal (**a**), dorsoposterior (**b**) and left lateral views. **d**, detail of exits of the nerve in anterolaterodorsal view (corresponding approximately to the frame in **c**); **e**, position of the fossil in a schematic reconstruction of the braincase of a mawsoniid coelacanth (modified from Maisey, 1986). Abbreviations: d.s, dorsum sellae; f.s.o.sc, foramen for the supraorbital sensory canal; f.s.opth, foramen for the superficial ophthalmic nerve; f.III, foramen for the oculomotor nerve; f.IV, foramen for the trochlear nerve (IV); ant. pr, antotic process; Par, parasphenoid; pr.con, processus conectens; pPa, posterior parietal; sph.c, sphenoid condyle; spt.fos, suprapterygoid fossa; v.pr.pPa, ventral process of the parietal posterior.

Evidence of embryos or newborn *Trachymetopon*

Two small basisphenoids of coelacanth (Fig. 3; MPV 2020.1.13a & b) were found by Elisabeth and Gérard Pennetier in the Callovian beds from the Vaches Noires. These specimens were donated to the Paléospace Muséum, France.

The anatomical organization of the internal face of the ossifications (Appendix 3), with fossae supporting the presence of a compact pituitary gland, indicates by comparison with the development of brain in fetus and pups of *Latimeria*[31], that they belong to very young individuals rather than to adult specimens of a small species. Their overall anatomy, close to the basisphenoid of the giant specimen, allows referring them to pups of *Trachymetopon* sp. of approximately 50 and 38 centimeters in total length. Both specimens consist of ventral part of the basisphenoids only, i.e. the paired processus connectens connected via a bony surface against which abutted the notochord, the paired sphenoid condyles and the dorsum sellae in one specimen. In the largest specimen (MPV 00.1.13a), the sphenoid condyles are widely separated and not very protruding, probably for preservational reasons. The smallest specimen

(MPV 00.1.13b) is better preserved than the larger one. There are no visible breaks of bone laterally, and we suppose that the lateral sides of both specimens were not ossified at these stages. The internal side of the both specimens shows well-marked reliefs. On the anterior part of the bone, the ventral side and the lateral sides bear strong grooves for suturing with the parasphenoid.

Hypophyseal development in *Trachymetopon*: In the adult *Latimeria*, the brain occupies about 1% of the space, and the ventral floor of the basisphenoid is dug by the pituitary fossa (pit. fos), which accommodates the enlarged anterior portion of pars distalis (adenohypophysis) of the pituitary gland, while the posterior part of the gland, including the bipartite pars intermedia is located much more posteriorly beneath the optic chiasm in the otico-occipital portion of the braincase[32,11]. Dutel et al.[31] showed that the pituitary gland underwent strong modifications during ontogeny in *Latimeria*. At fetal stage, the brain is proportionally very large and occupies both ethmosphenoid and otico-occipital cavities, and the pituitary gland is compact and lies under the diencephalon. During growth, the gland shifts towards the telencephalon when the brain is being concentrated in the posterior part of the cavity, while the anterior extremity of the pars distalis remains at the level of the basisphenoid and connects to the pars intermedia by the hypophyseal duct. The buccohypophysal canal (b.h.c) closes early during ontogeny[33]. Based on the observation in *Latimeria*, we consider that both small basisphenoid belong to pups of *Trachymetopon*, and we interpret the reliefs on their floor as following: a posterior bilobate fossa accommodated the bipartite pars intermedia of the pituitary gland, while a median deep cavity situated just anteriorly corresponds to the pituitary fossa of adult coelacanths, i.e. it accommodated the anterior part of the pars distalis (the adenohypophysis). Both pars are still close to each other because of the early stage of development. A groove anterior to the pituitary fossa accommodated the remnant of the buccohypophyseal canal.

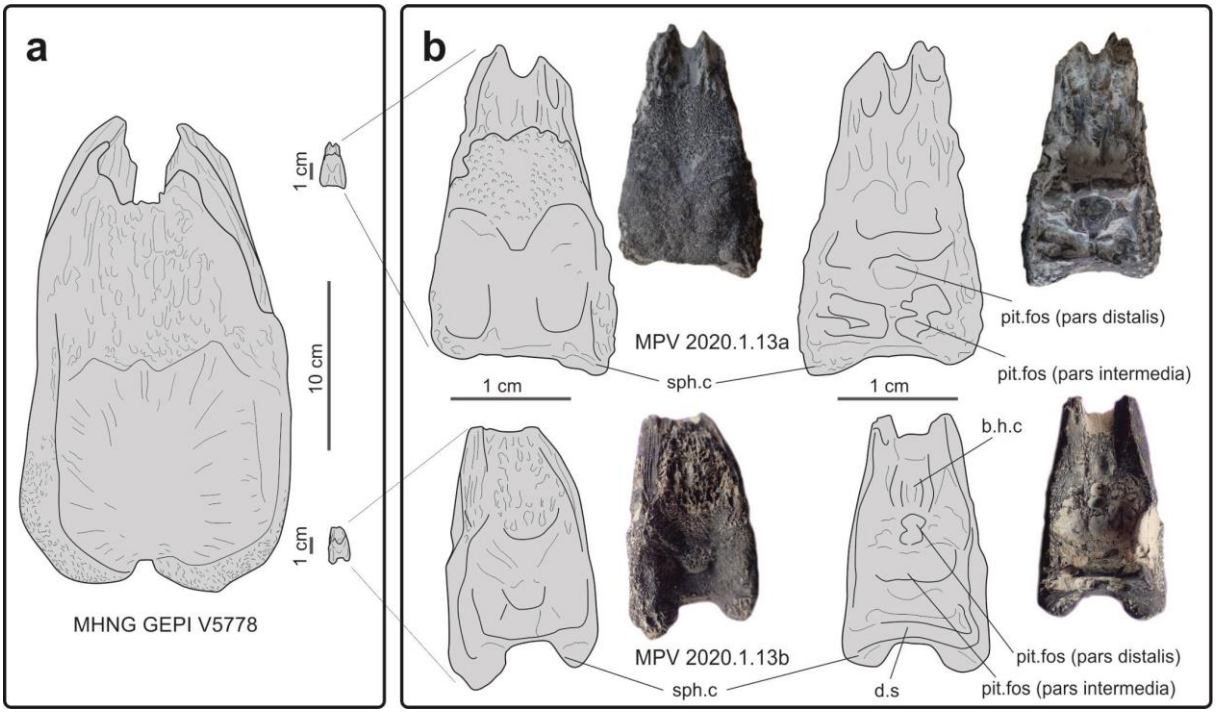

Figure 3

Basisphenoids of embryos or newborns of *Trachymetopon* sp. from Callovian beds from the Vaches Noires. **a**, Comparison of the giant form (MHNG GEPI V5778) with basisphenoids of embryos or newborns (MPV 2020.1.13); **b**, details of the parasphenoids of the embryos or newborns (MPV 2020.1.13a and MPV 2020.1.13a) in ventral (left) and dorsal (right) views. Abbreviations: b.h.c, buccohypophysal canal; d.s, dorsum sellae; pit. fos, pituitary fossa; sph.c, sphenoid condyle.

Trachymetopon stratigraphical range

So far, the genus *Trachymetopon* is known in the Early and Middle Jurassic of Europe, but new data require re-evaluation of this stratigraphic range. *Trachymetopon liassicus* from the Toarcian (Early Jurassic) of Holzmaden, Germany, was named and described by Hennig[30] and revised by Dutel et al.[29], who referred it to the family Mawsoniidae on the basis of a cladistic

analysis. The holotype is a complete and articulated specimen of 1.6 meter in length, i.e. in the length range of the extant *Latimeria*. *Trachymetopon* was then discovered in the Middle Jurassic with giant forms discovered in Callovian strata in Normandy, France, described by Dutel et al.[25] and in the present study.

In addition to this material, the Etches collection Museum at Kimmeridge, Dorset, UK, houses skull elements of a coelacanth from the Kimmeridgian (K785) that reached about 1.5 meters in length compared to skeletal proportions of the complete type specimen. It consists of an angular, a quadrate, a metapterygoid and partial pterygoid, of a paired ceratohyals, of a cleithrum and indeterminate bones. The shape and ornamentation of the angular, and the proportion of the palatoquadrate are reminiscent to mawsoniids, and more specifically *Trachymetopon*. It is referred here with caution to *Trachymetopon* sp.

The holotype and only known specimen of *"Macropoma" substriolatum* (SMC J27415; Fig. 4) from the Kimmeridgian of Cottenham, Cambridgeshire, UK, was originally included in the genus *Macropoma* by Huxley[8], then *Coccoderma* by Reis[34] and Woodward[35], and eventually brought closer to *Holophagus* by Forey[11]. In this specimen, the supratemporals appear to be restricted to the posterior lateral margin of the postparietal shield, and extend posteriorly creating a space that was occupied by the extrascapulars (not preserved, or only as fragments), like in mawsoniids and some other coelacanth genera. The strong ornamentation of the skull roof with conspicuous ridges and grooves is another mawsoniid characters. Similar to *Trachymetopon*, the quadrate is massive, broad and has a convex anterior margin, the angular is long and low with a straight outline. The cheek is composed of a lachrymojugal, a postorbital, a squamosal and a preopercle, which are all thick and proportionally large bones with coarse ornamentation, as in mawsoniids. A difference with *T. liassicum* is that some bones strongly ornamented in the latter species (e.g., the postparietal, the angular, the opercle) are almost smooth with only a dense pattern of small pits in *T. substriolatum*. However, these

parts of the specimen are the most exposed ones and we suspect that they were worn possibly before fossilization or, more probably, once the fossil was exposed to the surface. The specimen can be referred to a mawsoniid, and we refer it provisionally to *Trachymetopon*. Based on our model, this individual was small, about 60 cm in length.

Based on this short review, we consider with confidence that the stratigraphic range of *Trachymetopon*, previously restricted to the Early and Middle Jurassic, extends to the Late Jurassic.

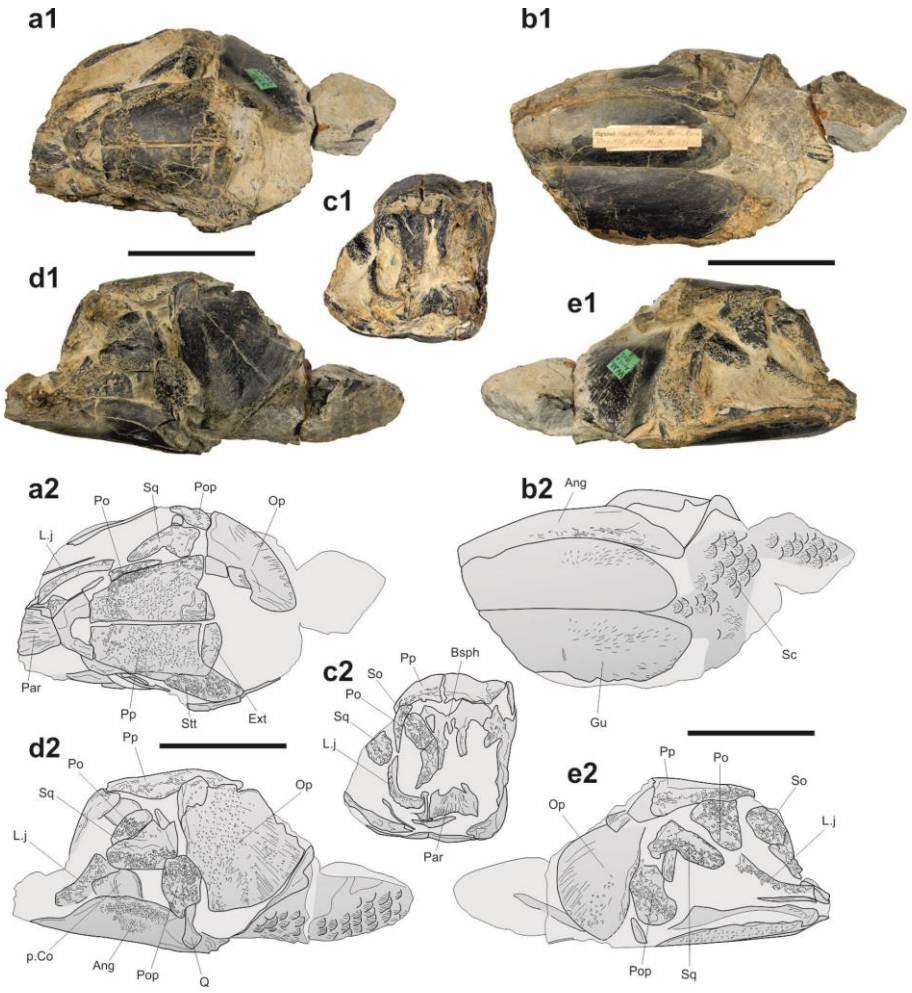

Figure 4

Trachymetopon ("*Macropoma*") *substriolatum* (holotype, SMC J27415) from the Kimmeridgian of Cottenham, Cambridgeshire. Photograph (1) and semi-interpretative

291 drawings in dorsal (**a**), ventral (**b**), anterior (**c**), left lateral (**d**) and right lateral (**e**) views. Scale
292 bars = 50 mm. Abbreviations: Ang, angular; Bsph, basisphenoid; Ext, extrascapular; Gu,
293 gular; L.j, lachrymojugal; Op, opercle; Par, parasphenoid; p.Co, principal coronoid; Pop,
294 postparietal; Pp, postparietal; Po, postorbital; Q, quadrate; Sc, scale; So, supraorbital; Sq,
295 squamosal; Stt, supratemporal.

296

297 **A Review of giant Mesozoic coelacanths**

298 First remains of giant mawsoniids from the Early Cretaceous of Brazil were originally
299 misinterpreted as belonging to a giant pterosaur by Woodward[36] because of the peculiar
300 biconvex articular condyle of the quadrate. This author then recognized his error with more
301 complete material from the Recôncavo Basin, Brazil, that he named *Mawsonia gigas* based on
302 its obvious large body size[37]. Based on our model (see Material & Methods), the body length
303 of the holotype individual reached 3.1 meters in length. *Mawsonia* bones were later found in
304 various Early Cretaceous South American basins mostly Brazil but also Uruguay[38,39], mainly
305 represented by fragmentary elements corresponding to middle-sized individuals, but also to
306 giant ones. One specimen coming from the Neocomian of Bahia is an articular head of a
307 quadrate (DGM 1.048-P) and corresponds to an individual of 6.3 m in length according to
308 Carvalho & Maisey[40]. Examination of this specimen by one of us (LC) and estimation based
309 on our model indicates a total body length of 5.3 m (Fig. 5). Medeiros et al. 41 recorded from
310 the Laje do Coringa flagstone, Alcântara Formation in northeastern Brazil, a fragment of a
311 large pterygopalatine comprising the quadrate, the metapterygoid and a piece of the pterygoid
312 (UFMA 1.40.468). Based on our model, this specimen was 4.9 meters long. African
313 Cretaceous mawsoniids also reached meters-long sizes[23,24], but never as large as
314 *Trachymetopon* or as South American mawsoniids. The sister genus of *Mawsonia* is
315 *Axelrodichthys*, which lived for part of its time interval in sympatry with *Mawsonia* in

316 Brazil[42], and extends to the Late Cretaceous in Europe with smaller forms[43]. In Africa
317 *'Mawsonia' lavocati* has been referred to *Axelrodichthys* by Fragoso et al.[44], and remains of
318 this species from the Kem Kem Group in Morocco indicate individuals up to 3.5 meters
319 long[45].

320 Dutel et al.[25] referred an isolated palatoquadrate (MPV 2012.1.1) found in the Callovian
321 (Middle Jurassic) of the Vaches Noires, France, to *Trachymetopon* sp. This specimen
322 corresponds to a large individual estimated to reach 4 meters in length. In addition to this
323 large pterygoid, we mention here a large ceratohyal (MPV 2014.2.344) found in the same
324 Callovian beds of the Vaches Noires, housed in the Paléospace Museum (Fig. 5). We estimate
325 that this bone corresponds to an individual slightly larger than the one represented by the
326 pterygoid, i.e. 4.4 meters in length.

327 Among the latimeriids, *Megalocoelacanthus dobiei* is a giant species from the Late
328 Cretaceous of North America known by disarticulated and mainly known by cranial elements.
329 Several estimates of body size have been proposed, i.e. between 3.8 and 4.0 m for the
330 holotype specimen (CCK 88-2-1) calculated by Schwimmer[26] and between 2.3 and 3 m for
331 another specimen (AMNH FF 20267) calculated by Dutel et al.[27]. Based on the basisphenoid
332 of the holotype and comparison with to the body proportions of *Latimeria*, we obtained a total
333 length of 3.5 m for the latter specimen.

334 The body length estimates for the largest known specimens are summarized in Table 1.

335

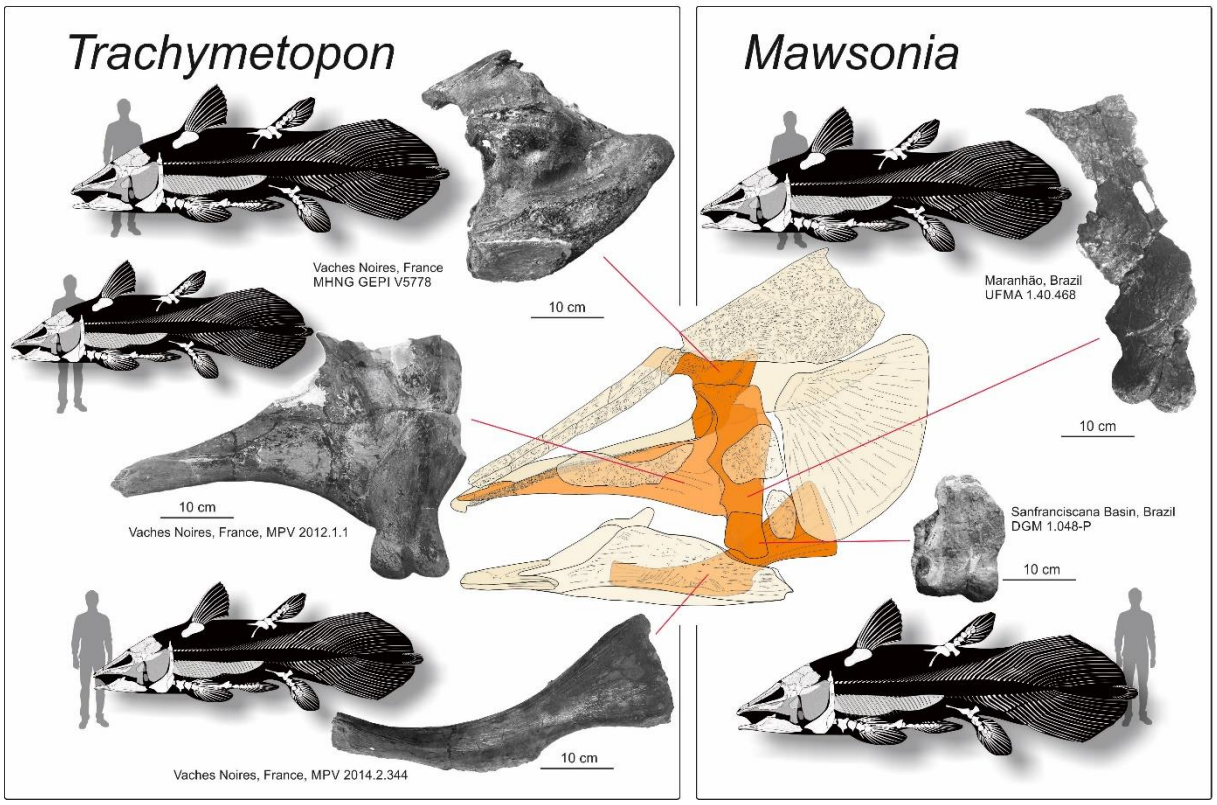

336

337 **Figure 5**

338 Fragmentary elements from the giant specimens of the Jurassic *Trachymetopon* and the

339 Cretaceous *Mawsonia*. Human silhouettes corresponds to 1.8 m.

340

Trachymetopon spp.		*Mawsonia gigas*		*Axelrodichthys lavocati*		*Megalocoelacanthus dobei*	
specimens	B.L.	specimens	B.L.	specimen	B.L.	specimen	B.L.
MHNG GEPI V5778	5.0	DGM 1.048-P	5.3	UMI-1	3.5	CCK 88-2-1	3.5
MPV 2014.2.344	4.4	UFMA 1.40.468	4.9				
MPV 2012.1.1	4.0						

341 **Table 1**

342 Calculated body length (B.L., in meters) for some of the largest specimens of *Trachymetopon*

343 spp., *Mawsonia gigas*, *Axelrodichthys lavocati* and *Megalocoelacanthus dobei*.

344

345 **Body size evolution and disparity in coelacanths**

346 Linear regression analysis between coelacanth logtransformed body length and time
347 expressed in time bins spanning the Devonian-Cretaceous interval shows a statistically
348 significant positive correlation (r=0.42963; p<0.0001), indicating a general trend for body size
349 increase over time in Actinistia.

350 We computed the coefficient of variation to quantify coelacanth body size disparity across 17
351 time bins spanning the Devonian-Paleocene interval, and used actinopterygians for
352 comparison. Actinopterygians were chosen because their time range is comparable to that of
353 coelacanths, and because of their enormous taxic diversity, which makes them representatives
354 of the changes in body length disparity through time in about half of the vertebrate diversity.
355 Our results (Fig. 6A) indicate that body size disparity is globally lower in coelacanths, with
356 the exception of the earliest stages of their evolutionary history. However, the ray-finned fish
357 taxic diversity is tremendously higher than that of coelacanths over the vast majority of their
358 evolutionary history (Fig. 6A), which tends to make direct comparison of disparity
359 misleading. Once standardized by taxic diversity, the per genus body size disparity patterns
360 differ drastically (Fig. 6B). Coelacanths display a much higher per genus disparity than
361 actinopterygians by several orders of magnitude throughout most of their evolutionary
362 history, excepted in the late Carboniferous where actinopterygians show a high per genus
363 disparity and in the Permian, where both clades present roughly similar disparity values.

364

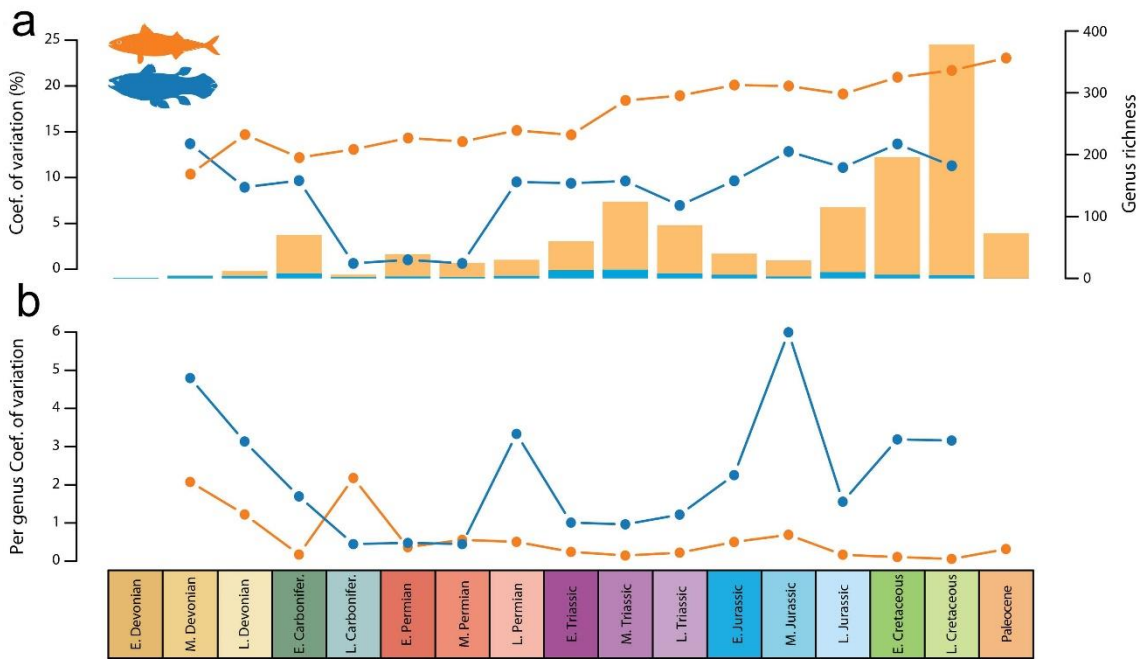

Figure 6

a, range-through genus richness (histograms) and disparity expressed by the coefficient of variation (dots and lines); **b**, per genus coefficient of variation, which is the coefficient of variation standardized by taxic diversity. Orange, Actinopterygii; blue, Actinistia.

Discussion

The new fragmentary remains of *Trachymetopon* described here, and the body size reassessment of Jurassic and Cretaceous mawsoniids indicate the presence of individuals reaching or exceeding 5 meters in total body length during the Jurassic and Cretaceous. By comparison, among the actinopterygians living from the Devonian to the Paleocene, the only genera which approach or exceed *Mawsonia* and *Trachymetopon* in length are two giant marine planktivorous pachycormiforms, the Jurassic *Leedsichthys* (16 m) and the Cretaceous *Bonnerichthys* (6.1 m), as well as the Late Cretaceous to Recent *Acipenser* (5 m). Among the

extant ray-finned fish, the only longest species include another chondrostean, *Huso huso* (7.2 m) and the Atlantic blue marlin, *Makaira nigricans* (5 m), as well as the oarfish *Regalecus glesne* (13.7 m) but the latter has a compressed and slender profile very different from the other fish compared, all more or less fusiform shaped. Thus, the two genera of mawsoniid coelacanths are among the ten largest bony fish that have ever lived. Interestingly, one of these giant coelacanths, *Trachymetopon*, lived in sympatry in the European Callovian Sea with the largest ray-finned fish that ever lived, *Leedsichthys*[46].

Fifteen genera of coelacanths are known in the Jurassic and Cretaceous, i.e. contemporaneous genera of the giant *Trachymetopon* and *Mawsonia*. They were medium-sized fish, but proportionately small compared to the two giants, with seven genera whose body length did not exceed 0.5 meters *(Reidus, Swenzia, Macropomoides, Coccoderma, Atacamaia, Undina,* and *Lualabaea*). The smallest known coelacanth genera lived mainly in the Paleozoic (*Holopterygius, Lochmocercus, Hadronector,* and *Youngichthys*), then in the Triassic (*Piveteauia* and *Chaohuichthys*). The general mean increase in body size in this lineage is demonstrated by the correlation between body size and time, which confirms the Cope's rule previously observed in many clades[2]. Such a trend is not observed in actinopterygians as a whole, but is present in most of the main clades taken separately[47], probably because testing the Cope's rule gives contrasting results depending on the taxonomic level used[48]. From this aspect, the coelacanths do not deviate from this general macroevolutionary trend.

Our analyses of the evolution of body size disparity in coelacanths indicate high disparity from the Late Permian onward compared with actinopterygians. Although this pattern is not visible based on raw disparity values (Fig. 6a), it is clearly noticeable when disparity is standardized by taxic diversity, which allows to fit the much higher finned-ray diversity to the depleted coelacanth clade (Fig. 6b). A decrease is visible for both clades in the Late Jurassic, possibly caused by the Lagerstätten effect detected in the fossil record of ray-finned fish at

405 this time[49] which alters the measure of disparity by preserving a greater diversity and more
406 complete specimens[50]. We also note that the variance in body size of ray-finned fish steadily
407 increases over time when the index is taken raw, but when adjusted for diversity, the variance
408 in body size is very stable during the Permian-Paleocene interval, possibly indicating that the
409 body size ecospace was fulfilled during this time interval.

410 Previous studies have demonstrated that the coelacanth morphological disparity, whether
411 measured by morphospace occupation[51] or by computation of new discrete characters in a
412 phylogenetic framework[9,10,11,12,14], shows a burst at the origin of the group in the Devonian –
413 Carboniferous. These studies confirmed the early burst (EB) model first proposed by
414 Simpson[52], which was then verified at a large scale among animal clades[53,54,55], and
415 demonstrated more specifically in the ichthyosaurs[56]. The same trend is observed here for
416 body size disparity in the early evolutionary history of the coelacanths. However, the
417 coelacanth pattern differs from that of other clades in that their body size disparity did not
418 decrease through time, contrary to what is observed in the morphological evolution of
419 ichthyosaurs for instance[56]. Instead, the evolution of the coelacanth body size disparity tended
420 to increase until the late Cretaceous, then this evolutionary trend remains unknown due to the
421 lack of fossils in the Cenozoic. Interestingly, our analyses indicate that the evolution of body
422 size disparity in coelacanths is decoupled from the observed trends in taxic diversity
423 (Pearson's product-moment correlation: 0.3450382; p-value = 0.2078). Such a decoupling
424 between morphological disparity and diversity after the initial radiation of a clade has been
425 reported on many instances for various groups based on fossil evidence[57,58], indicating that
426 taxic diversity and disparity may be controlled by different factors (but see[3,4]). However, the
427 post-Carboniferous variations in body size disparity through time among coelacanths does not
428 mirror those of morphological evolution for this clade either (e.g.[9,10,11]). Those studies on
429 morphological evolution indicate a steady drop from the Carboniferous until the Cretaceous

with some exception such as the aberrant *Foreyia* from the middle Triassic[59], which is in sharp contrast with the pattern of body size disparity presented in Fig. 6. This indicates that body size might not be an accurate proxy for reflecting morphological evolution and/or disparity. Alternatively, the decoupling between the disparity in body size and the taxic diversity observed in the coelacanth clade may represent an exception among vertebrates corresponding to an additional specific evolutionary trait associated with their status as "living fossils".

Underwater observations in situ[60,61] and gill surface measurements[62,63,64] of *Latimeria* all indicate a very low metabolic rate in this fish. Based on Kleiber's law stating that large animals have a proportionately lower metabolic rate than small ones, and although we cannot say whether a low metabolic rate is a cause or consequence of a large body size, the low rate observed in *Latimeria* can be considered as a trait inherited from the common ancestor of the latimeroids (mawsoniids plus latimeriids), which is associated in an indeterminate way to the gigantism of *Mawsonia* and *Trachymetopon*, and to the large size of *Axelrodichthys* and *Megalocoelacanthus*. The recent study[65] of the genome of the giant whale shark (*Rhincodon typus*) and a comparison of genomic and physiological features of a set of 83 animals revealed several correlations between these life traits. In particular, these authors detected a negative correlation between length of introns in the genome and metabolic rate, and a positive correlation between length of introns and body size. *Latimeria* has proportionally long intron length ([65], figures 1E, S3), making its clade prone to evolve toward large body size.

New fossil discoveries and an examination of the body size of coelacanths through time confirm that the evolutionary history of these fish is in agreement with two major macroevolutionary trends widely observed in animal evolution, namely an early burst in their morphological disparity (previously demonstrated) and a gradual increase in body size

455 through (Cope/Depéret's rule), but they also deviate from two other macro-evolutionary
456 trends, that is, their variations in body size disparity are not linked with taxic diversity nor
457 with morphological evolution. The genomic characteristics, the long intron length and the
458 physiological characteristics, the low metabolic rate of the extant *Latimeria* constitute a
459 favorable ground for the evolution towards gigantism in this clade.

460

461 Material and methods

462

463 Microplalaeontological preparation

464 Microfossils have been extracted from a very small amount of rock residue retrieved from the
465 preparation of the coelacanth bone. Due to the strong induration of the sediment, extraction of
466 microfossils, unsuccessful with traditional washing methods (e.g.[66]), have then been done by
467 acetolysis[67].

468

469 Body size reconstruction

470 The model used to reconstruct the body length in Fig. 5 is based on the reconstruction of
471 *Axelrodichthys araripensis* by Forey ([11], figure 11.3), itself based on the reconstruction of
472 Maisey[42] with some additions. As far as the material allows to assess, there are no major
473 differences in body proportions between *Axelrodichthys*, *Trachymetopon* and *Mawsonia*. Note
474 that our model is based on individuals much smaller than the individuals studied here, and it is
475 possible that allometric growth may alter the calculation of body size estimates. However,
476 McAllister and Smith[68] showed that in *Latimeria chalumnae* the length of the head, from the
477 snout to the posterior end of the operculum, grows isometrically compared to the standard

478 length. If, anyway, allometric growth was present in mawsoniids, it means that our body size
479 reconstructions are underestimated because the allometry in fish, as in most vertebrates,
480 involved a proportionately larger head in young individuals than in older and larger ones.

481

482 **Stratigraphical ranges and body size dataset**

483 We gathered data on the fossil record (first and last occurrences) of each of the 63 coelacanth
484 genera from the Devonian to the Paleocene. We further compiled the maximum body length
485 for each genus based on the literature and/or on direct measurements of complete specimens
486 or based on estimates for partial specimens. For species known by isolated skulls only, we
487 multiplied the skull length (snout to posterior margin of the opercle) by 4.14, a ratio
488 calculated on the basis of a sample of complete specimens of various species. For comparison
489 purpose, we also gathered data for the actinopterygians. These are based on an update of
490 Guinot & Cavin[47,69], with new information from Sallan & Coates[70] for Devonian taxa,
491 Romano et al.[71] for Permo-Triassic taxa and Alberts et al.[72], complemented by extensive
492 literature review. We used total length for both actinistian and actinopterygian genera. When
493 only standard lengths were available for ray-finned fishes, we multiplied them by 1.2 for
494 getting the total length, a ratio calculated on the basis of a large sample of taxa known by
495 complete specimens. When different sizes were available for one species, we selected the
496 longest one. When several species are known for a genus, we selected the longest one.

497

498 **Stratigraphical ranges and body size analyses**

499 We used the coefficient of variation to quantify body size disparity across time bins
500 throughout the Devonian-Paleocene interval. The coefficient of variation is expressed here in
501 percent, as follows: $Cv = \frac{\sigma}{\mu} * 100$ where σ is the standard deviation and μ is the mean of the

body size values. We computed the coefficient of variation for each of the 17 time bins, which represent geological Epochs. Because disparity values can be influenced by taxic diversity, we further divided values of *Cv* in each time bin by the corresponding value of taxic diversity (computed by range-through), thus providing a per genus coefficient of variation standardized by taxic diversity. This allowed comparisons to be made between disparity values of clades that differ drastically in taxic diversity, such as actinistians and actinopterygians. Body length values were log-transformed prior to the analyses.

References

[1] Bokma, F. et al. Testing for Depéret's rule (body size increase) in mammals using combined extinct and extant data. *Syst. Biol*. **65**, 98-108. (2016).

[2] Heim, N. A., Knope, M. L., Schaal, E. K., Wang, S. C. & Payne, J. L. Cope's rule in the evolution of marine animals. *Science* **347**, 867-870. (2015).

[3] Rabosky, D. L. et al. Rates of speciation and morphological evolution are correlated across the largest vertebrate radiation. *Nat. commun*. **4**, 10.1038/ncomms2958 (2013).

[4] Cooney, C. R. & Thomas, G. H. Heterogeneous relationships between rates of speciation and body size evolution across vertebrate clades. *Nat. Ecol. Evol.* **5**, 101-110 10.1038/s41559-020-01321-y (2020).

524 [5] Lloyd, G. T. Journeys through discrete-character morphospace: synthesizing phylogeny,
525 tempo, and disparity. *Palaeontology* **61**, 637-645. (2018).

526 [6] Darwin, C. *On the Origin of Species by Means of Natural Selection, or the Preservation of*
527 *Favoured Races in the Struggle for Life*. John Murray, p. 502 (1859).

528 [7] Toriño, P. A comprehensive phylogenetic analysis of coelacanth fishes (Sarcopterygii,
529 Actinistia) with comments on the composition of the Mawsoniidae and Latimeriidae:
530 Evaluating old and new methodological challenges and constraints. *Hist. Biol*. In press.

531 [8] Huxley, T.H. Illustrations of the structure of the crossopterygian ganoids. Figures and
532 descriptions illustrative of British organic remains. *Mem. Geol. Survey U.K, Lond.*, 1-44
533 (1866).

534 [9] Schaeffer, B. Rates of evolution in the coelacanth and dipnoan fishes. *Evolution* **6**, 101-
535 111 (1952).

536 [10] Cloutier, R. Patterns, trends, and rates of evolution within the Actinistia. in *The biology*
537 *of* Latimeria chalumnae *and evolution of coelacanths.* Springer, 23-58 (1991).

538 [11] Forey, P. *History of the Coelacanth Fishes*. Chapman and Hall, London (1998).

539 [12] Schultze, H. P. Mesozoic sarcopterygians. in *Mesozoic fishes 3*, Dr Pfeil Verlag, 463-492
540 (2004).

541 [13] Zhu, M., Yu, X., Lu, J., Qiao, T., Zhao, W. & Jia, L. Earliest known coelacanth skull
542 extends the range of anatomically modern coelacanths to the Early Devonian. *Nat.*
543 *Commun.* **3**, 1-8. (2012).

544 [14] Cavin, L. & Guinot, G. Coelacanths as “almost living fossils”. *Front. Ecol. Evol.* **2**, 49.
545 (2014).

546 [15] Bennett, D. J., Sutton, M. D. & Turvey, S. Quantifying the living fossil concept.
547 *Palaeontol. Electronica*, (21.1. 14A) (2018).

548 [16] Nikaido, M. et al. Genetically distinct coelacanth population off the northern Tanzanian
549 coast. *Proc. Natl. Acad. Sci. U.S.A.* **108**, 18009-18013 (2011).

550 [17] Lampert, K. P. et al. Population divergence in East African coelacanths. *Curr. Biol*. **22**,
551 R439-R440 (2012).

552 [18] Kadarusman et al. A thirteen-million-year divergence between two lineages of
553 Indonesian coelacanths. *Sci. Rep*. **10**, 1-9 (2020).

554 [19] Nikaido, M. et al. Coelacanth genomes reveal signatures for evolutionary transition from
555 water to land. *Genome research* **3**, 1740-1748 (2013).

556 [20] Amemiya, C. T. et al. Complete HOX cluster characterization of the coelacanth provides
557 further evidence for slow evolution of its genome. *Proc. Natl. Acad. Sci. U.S.A.* **107**,
558 3622-3627. (2010).

559 [21] Amemiya, C. T. et al. The African coelacanth genome provides insights into tetrapod
560 evolution. *Nature* **496**, 311-316 (2013).

561 [22] Woodward, A. S. Notes on some Upper Cretaceous Fish remains from the Province of
562 Sergipe and Pernambuco, Brazil. *Geol. Mag*. **4**, 193–197 (1907).

563 [23] Wenz, S. Un coelacanthe géant, *Mawsonia lavocati* Tabaste, de l'Albien-base du
564 Cénomanien du sud marocain. *Ann. Pal. (Vert.)* **67**, 1-20 (1981).

565 [24] Yabumoto, Y. & Uyeno, T. New materials of a Cretaceous coelacanth, Mawsonia
566 lavocati Tabaste from Morocco. *Bull. Natn. Sci. Mus. [Tokyo], Ser. C* **31**, 39-49 (2005).

567 [25] Dutel, H., Pennetier, E. & Pennetier, G. A giant marine coelacanth from the Jurassic of
568 Normandy, France. *J. Vertebr. Paleontol*. **34**, 1239-1242 (2014).

569 [26] Schwimmer, D.R. Giant fossil coelacanth from the Late Cretaceous of the Eastern
570 United-States. *Fernbank Magazine*, 24-30 (2002).

571 [27] Dutel, H., Maisey, J. G., Schwimmer, D. R., Janvier, P., Herbin, M. & Clément, G. The
572 giant Cretaceous coelacanth (Actinistia, Sarcopterygii) *Megalocoelacanthus dobiei*
573 Schwimmer, Stewart & Williams, 1994, and its bearing on Latimerioidei
574 interrelationships. *PLoS ONE* **7**, e49911 (2012).

575 [28] Rioult, M., Coutard, J.-P., de La Quérière, P., Helluin, M., Larsonneur, C. & Pellerin, J.
576 Notice explicative de la feuille de Caen à 1/50000. Editions du BRGM, 1-104 (1989)

577 [29] Dutel, H., Herbin, M. & Clément, G. First occurrence of a mawsoniid coelacanth in the
578 Early Jurassic of Europe. *J. Vertebr. Paleontol*. **35**, e929581 (2015).

579 [30] Hennig, E. *Trachymetopon liassicum*, Ald., ein Riesen-Crossopterygier aus
580 Schwäbischem Ober-Lias. *Neues Jahrb. Geol. Palaontol. Abh*. **94**, 67–79 (1951).

581 [31] Dutel, H. et al. Neurocranial development of the coelacanth and the evolution of the
582 sarcopterygian head. *Nature* **569**, 556-559 (2019).

583 [32] Lagios, M. D. Evidence for a hypothalamo-hypophysial portal vascular system in the
584 coelacanth *Latimeria chalumnae* Smith. *Gen. Comp. Endocrinol*. **18**, 73-82 (1972).

585 [33] Khonsari, R. H. et al. The buccohypophyseal canal is an ancestral vertebrate trait
586 maintained by modulation in sonic hedgehog signaling. *BMC biology* **11**, 1-16 (2013).

587 [34] Reis, O.M. Die Coelacanthinen, rnit besonderer Beriicksichtigung der irn Weissen Jura
588 Bayerns vorkornrnenden Gattungen. *Palaeontographica* **35**, 1-96 (1888).

589 [35] Woodward, A.S. Catalogue of Fossil Fishes in the British Museum (Natural History).
590 Volume 2, xliv + 567 pp., London: British Museum (Natural History) (1891).

591 [36] Woodward, A. S. On the quadrate bone of a gigantic pterodactyl, discovered by Joseph
592 Mawson in the Cretaceous of Bahia. *Ann. Mag. nat. Hist*. **6**, 255-257 (1896).

593 [37] Mawson, J. & Woodward, A. S. On the Cretaceous formation of Bahia (Brazil), and on
594 vertebrate fossils collected therein. *Quart. J. Geol. Soc*. **63**, 128-138 (1907).

595 [38] Soto, M., De Carvalho, M. S., Maisey, J. G., Perea, D. & Silva, J. D. Coelacanth remains
596 from the Late Jurassic–? earliest Cretaceous of Uruguay: the southernmost occurrence
597 of the Mawsoniidae. *J. Vertebr. Paleontol*. **32**, 530-537 (2012).

598 [39] Toriño, P., Soto, M., Perea, D. & de Carvalho, M. S. S. New findings of the coelacanth
599 Mawsonia Woodward (Actinistia, Latimerioidei) from the Late Jurassic–Early
600 Cretaceous of Uruguay: Novel anatomical and taxonomic considerations and an
601 emended diagnosis for the genus. *J. S. Am. Earth Sci.* 103054 (2020).

602 [40] Carvalho de, M. S. & Maisey, J. G. New occurrence of *Mawsonia* (Sarcopterygii:
603 Actinistia) from the Early Cretaceous of the Sanfranciscana Basin, Minas Gerais,
604 southeastern Brazil. in *Fishes and the Break-up of Pangaea*, Geol. Soc., Lond. **295**,
605 109-144 (2008).

606 [41] Medeiros, M. A., Lindoso, R. M., Mendes, I. D. & de Souza Carvalho, I. The Cretaceous
607 (Cenomanian) continental record of the laje do coringa flagstone (Alcântara formation),
608 northeastern South America. *J. S. Am. Earth Sci.* **53**, 50-58 (2014).

609 [42] Maisey, J. G. Coelacanths from the lower cretaceous of Brazil. *Am. Mus. Novit*. **2866**, 1-
610 30 (1986).

611 [43] Cavin, L. et al. The last known freshwater coelacanths: new Late Cretaceous mawsoniid
612 remains (Osteichthyes: Actinistia) from southern France. *PLoS ONE*, **15**, e0234183
613 (2020).

614 [44] Fragoso, L. G.C., Brito, P. & Yabumoto, Y. *Axelrodichthys araripensis* Maisey, 1986
615 revisited. *Hist. Biol*. **31**, 1350-1372 (2019).

616 [45] Cavin, L., Boudad, L., Tong, H., Läng, E., Tabouelle, J. & Vullo, R. Taxonomic
617 composition and trophic structure of the continental bony fish assemblage from the
618 early Late Cretaceous of southeastern Morocco. *PLoS ONE* **10**, e0125786. (2015).

619 [46] Liston, J., Newbrey, M., Challands, T. & Adams, C. Growth, age and size of the Jurassic
620 pachycormid *Leedsichthys problematicus* (Osteichthyes: Actinopterygii). in *Mesozoic*
621 *Fishes 5*, Dr Pfeil, Verlag, 145-175 (2013).

622 [47] Guinot, G. & Cavin, L. Body size evolution and habitat colonization across 100 million
623 years (Late Jurassic–Paleocene) of the actinopterygian evolutionary history. *Fish Fish*.
624 **19**, 577-597 (2018).

625 [48] Hone, D. W. E. & Benton, M. J. Cope's Rule in the Pterosauria, and differing
626 perceptions of Cope's Rule at different taxonomic levels. *J. evol. biol*. **20**, 1164-1170
627 (2007).

628 [49] Cavin, L. The Late Jurassic ray-finned fish peak of diversity: biological radiation or
629 preservational bias. in *Origin and phylogenetic interrelationships of teleosts*. Dr Pfeil
630 Verlag, 111-121 (2010).

631 [50] Flannery Sutherland, J. T., Moon, B. C., Stubbs, T. L. & Benton, M. J. Does exceptional
632 preservation distort our view of disparity in the fossil record? *Proc. R. Soc. B* **286**,
633 201900 (2019).

634 [51] Friedman, M. & Coates, M. I. A newly recognized fossil coelacanth highlights the early
635 morphological diversification of the clade. *Proc. R. Soc. B* **273**, 245-250 (2006).

636 [52] Simpson, G. *Tempo and Mode in Evolution*. Columbia University Press, New York, NY
637 (1944).

638 [53] Hughes, M., Gerber, S. & Wills, M.A. Clades reach highest morphological disparity
639 early in their evolution. *Proc. Natl. Acad. Sci. USA* **110**, 13875– 13879 (2013).

640 [54] Wagner, P. J. Early bursts of disparity and the reorganization of character integration.
641 *Proc. R. Soc. Lond. Series B.* **85**, 0181604 (2018).

642 [55] Puttick, M. N. Mixed evidence for early bursts of morphological evolution in extant
643 clades. *J. evol. biol*. **31**, 50-515 (2018).

644 [56] Moon, B. C. & Stubbs, T. L. Early high rates and disparity in the evolution of
645 ichthyosaurs. *Commun. biology* **3**, 1-8 (2020).

646 [57] Hopkins, M. J. Decoupling of taxonomic diversity and morphological disparity during
647 decline of the Cambrian trilobite family Pterocephaliidae. *J. evol. biol*. **26**, 1665-1676
648 (2013).

649 [58] Ruta, M., Angielczyk, K. D., Fröbisch, J. & Benton, M. J. Decoupling of morphological
650 disparity and taxic diversity during the adaptive radiation of anomodont therapsids.
651 *Proc. R. Soc. Lond. Series B.* **280**, 20131071 (2013).

652 [59] Cavin, L., Mennecart, B., Obrist, C., Costeur, L. & Furrer, H. Heterochronic evolution
653 explains novel body shape in a Triassic coelacanth from Switzerland. *Sci. Rep*. **7**, 1-7
654 (2017).

655 [60] Fricke, H. & Plante, R. Habitat requirements of the living coelacanth *Latimeria*
656 *chalumnae* at Grande Comore, Indian Ocean. *Naturwissenschaften* 75, 149-151 (1988).

657 [61] Fricke H., Hissmann K., Home range and migrations of the living coelacanth *Latimeria*
658 *chalumnae*. *Mar. Biol*. **120**, 171-180 (1994).

659 [62] Hughes, G. M. On the respiration of *Latimeria chalumnae*. *Zool. J. Linn. Soc.* **59**, 195-
660 208 (1976).

661 [63] Hughes, G. M. Ultrastructure and morphometry of the gills of *Latimeria chalumnae*, and
662 a comparison with the gills of associated fishes. *Proc. R. Soc. Lond. Series B.* **208**, 309-
663 328 (1980).

664 [64] Hughes, G. M. The gills of the coelacanth, *Latimeria chalumnae* Latimeriidae. What can
665 they teach us? *Ital. J. of Zool.* **65**, 425-429 (1998).

666 [65] Weber, J. A. et al.. The whale shark genome reveals how genomic and physiological
667 properties scale with body size. *Proc. Natl. Acad. Sci. USA* **117**, 20662-20671 (2020).

668 [66] Kummel, B. & Raup, D (eds.) Handbook of Paleontological Techniques. W. H. Freeman
669 and Company, San Francisco and London, 1965. xiii + 852 pp (1965).

670 [67] Lirer, FA new technique for retrieving calcareous microfossils from lithified lime
671 deposits. *Micropaleontology* 365-369 (2000).

672 [68] McAllister, D. E. & Smith, D. Mensurations morphologiques, dénombrements
673 méristiques et taxonomique du coelacanthe, *Latimeria chalumnae*. *Nat. can*. **105**, 63-76
674 (1978).

675 [69] Guinot, G. & Cavin, L. 'Fish' (Actinopterygii and Elasmobranchii) diversification
676 patterns through deep time. *Biol. Rev*. **91**, 950-981 (2016).

677 [70] Sallan, L. C. & Coates, M. I. End-Devonian extinction and a bottleneck in the early
678 evolution of modern jawed vertebrates. *Proc. Natl. Acad. Sci. USA* **107**, 10131-10135
679 (2010).

680 [71] Romano, C. et al. Permian–Triassic Osteichthyes (bony fishes): diversity dynamics and
681 body size evolution. *Biol. Rev*. **91**, 106-147 (2016).

682 [72] Albert, J. S., Johnson, D. M. & Knouft, J. H. Fossils provide better estimates of ancestral
683 body size than do extant taxa in fishes. *Acta Zoologica* **90**, 357-384 (2009).

Acknowledgment

We thank Laurent Picot (Paléospace Muséum, Villers-sur-Mer, France), Elisabeth and Gérard Pénnetier (Association Paléontologique de Villers-sur-Mer, France) for access to specimens under their care, Matt Riley (Sedgwick Museum, Oxford, UK), Manuel Alfredo Araujo Medeiros (Universidade Federal do Maranhão, Brazil), Steve Etches and Carla Crook (The Etches Collection Museum of Jurassic Marine Life, Kimmeridge) for providing photographs of specimens under their care. We are grateful to Pierre-Alain Proz and Philippe Wagneur (Muséum d'histoire naturelle, Geneva) for the preparation and photograph of the specimen MHNG GEPI V5778, respectively. This paper is a contribution to the project "Evolutionary pace in the coelacanth clade: New evidence from the Triassic of Switzerland" (200021-172700) supported by the Swiss National Science Foundation.

Author contributions

L.C. designed the study and wrote the description of the fossil material, A.P. prepared and analyzed the micropaleontological data, C.F. collected the body size data and contributed to the description of the fossils, G.G. analyzed the body size data. All the authors contributed to the drafting of the last version of the text.

Competing interests

The authors declare no conflict of interest.

Figures

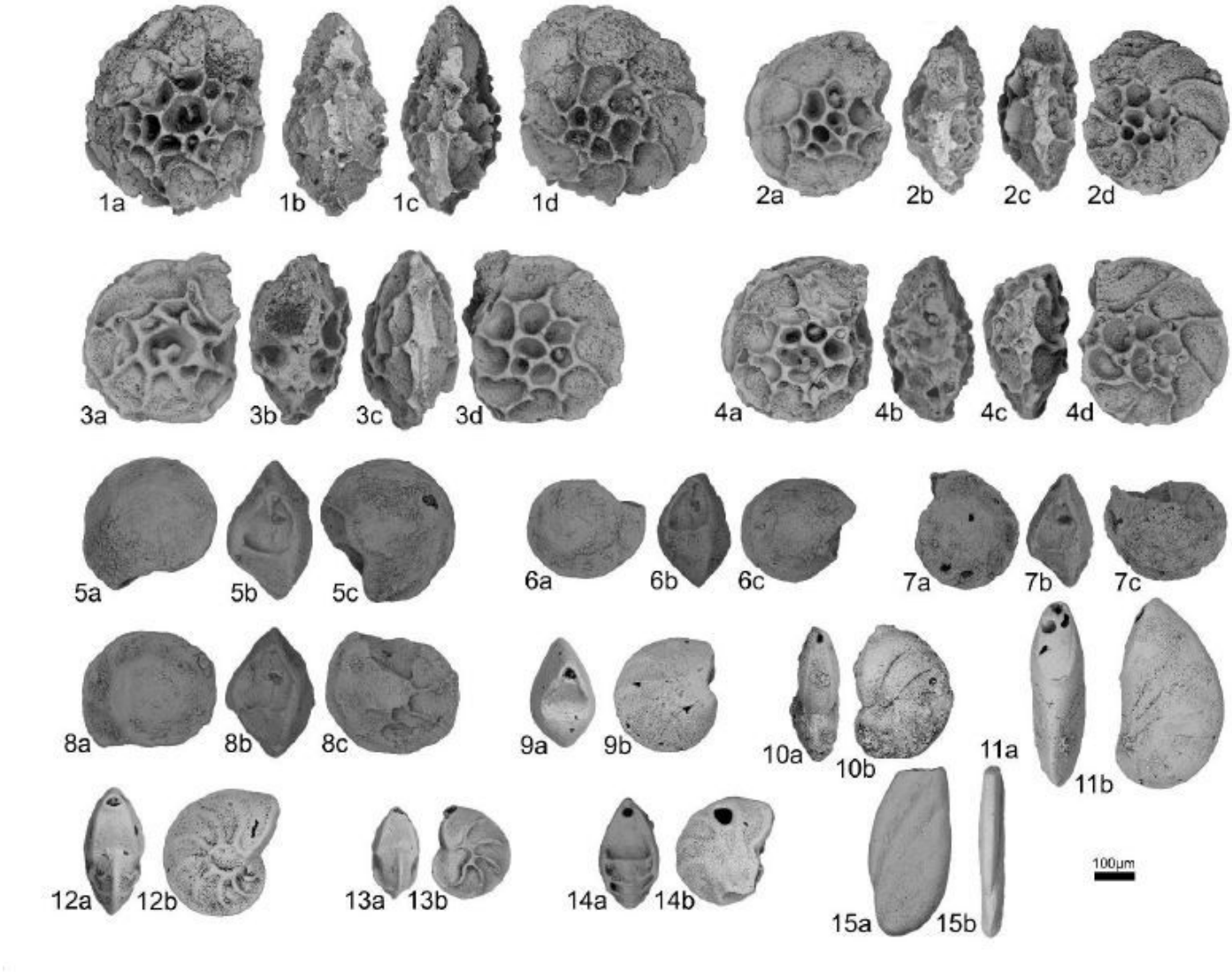

Figure 1

Foraminifera found in the matrix containing the fragment of the coelacanth skull (MHNG GEPI V5778). 1-4, Epistomina ex. gr. mosquensis Uhlig 1883, umbilical, apertural, carinal and spiral views; 5-8, Epistomina ex. gr. uhligi Mjatliuk 1953, spiral, apertural and umbilical views; 9-11, Lenticulina muensteri (Roemer 1839), apertural and lateral views; 12-13, Lenticulina quenstedti (Gümbel 1862), apertural and lateral views; 14, Lenticulina subalata (Reuss 1854), apertural and lateral views; 15, Planularia beierana (Gümbel 1862), lateral and apertural views.

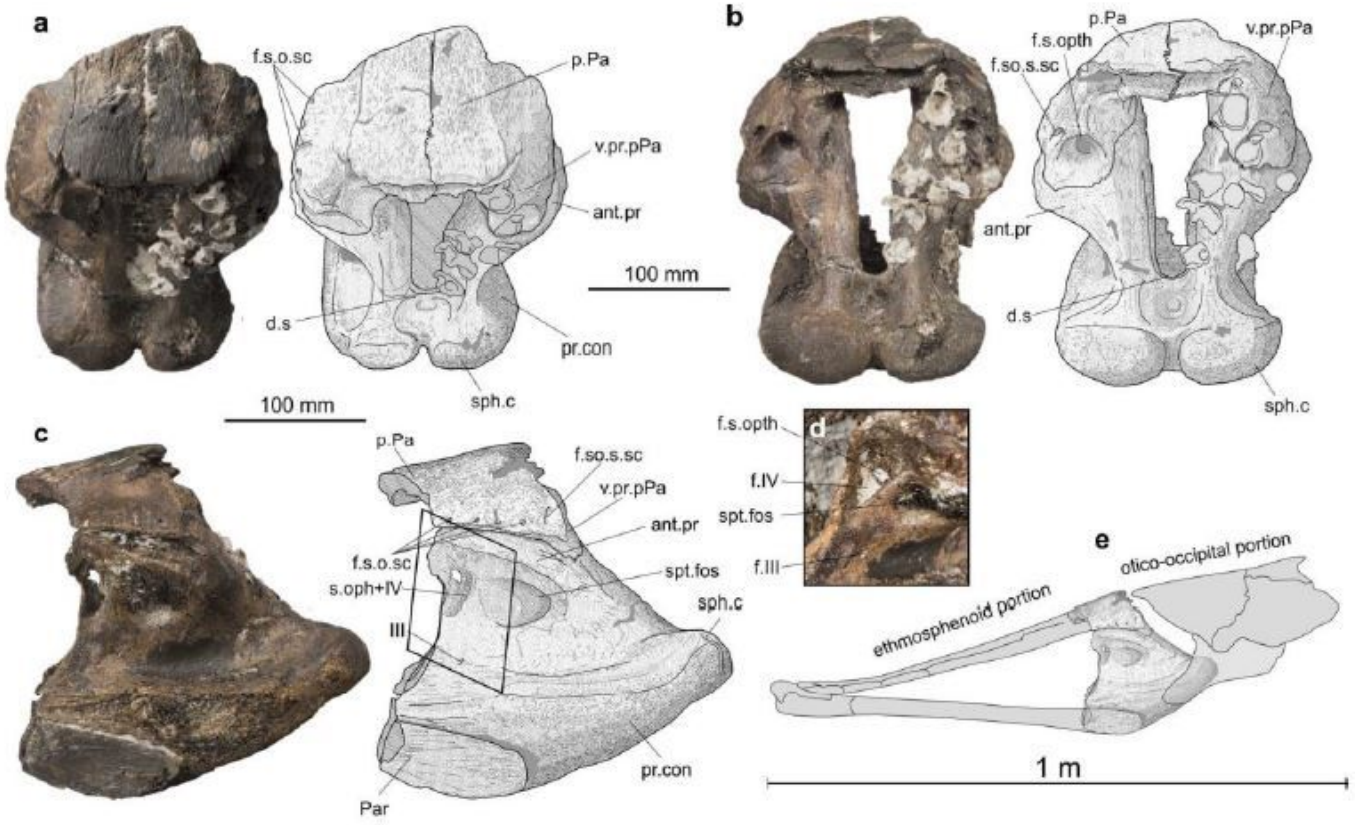

Figure 2

MHNG GEPI V5778. Trachymetopon sp. Basisphenoid with fragments of the posterior parietals and parasphenoid. Dorsal (a), dorsoposterior (b) and left lateral views. d, detail of exits of the nerve in anterolaterodorsal view (corresponding approximately to the frame in c); e, position of the fossil in a schematic reconstruction of the braincase of a mawsoniid coelacanth (modified from Maisey, 1986). Abbreviations: d.s, dorsum sellae; f.s.o.sc, foramen for the supraorbital sensory canal; f.s.opth, foramen for the superficial ophthalmic nerve; f.III, foramen for the oculomotor nerve; f.IV, foramen for the trochlear nerve (IV); ant. pr, antotic process; Par, parasphenoid; pr.con, processus conectens; pPa, posterior parietal; sph.c, sphenoid condyle; spt.fos, suprapterygoid fossa; v.pr.pPa, ventral process of the parietal posterior.

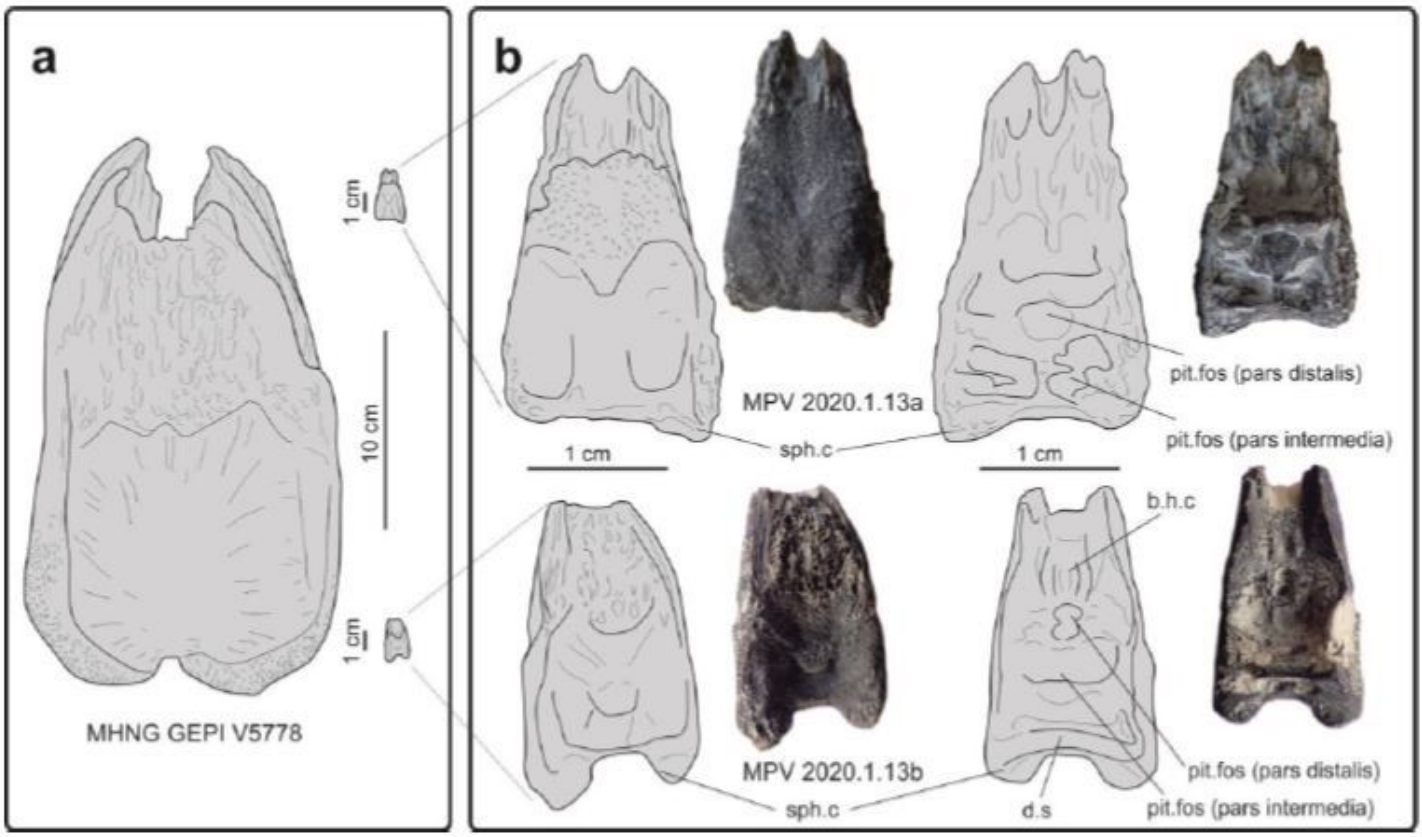

Figure 3

Basisphenoids of embryos or newborns of Trachymetopon sp. from Callovian beds from the Vaches Noires. a, Comparison of the giant form (MHNG GEPI V5778) with basisphenoids of embryos or newborns (MPV 2020.1.13); b, details of the parasphenoids of the embryos or newborns (MPV 2020.1.13a and MPV 2020.1.13a) in ventral (left) and dorsal (right) views. Abbreviations: b.h.c, buccohypophysal canal; d.s, dorsum sellae; pit. fos, pituitary fossa; sph.c, sphenoid condyle.

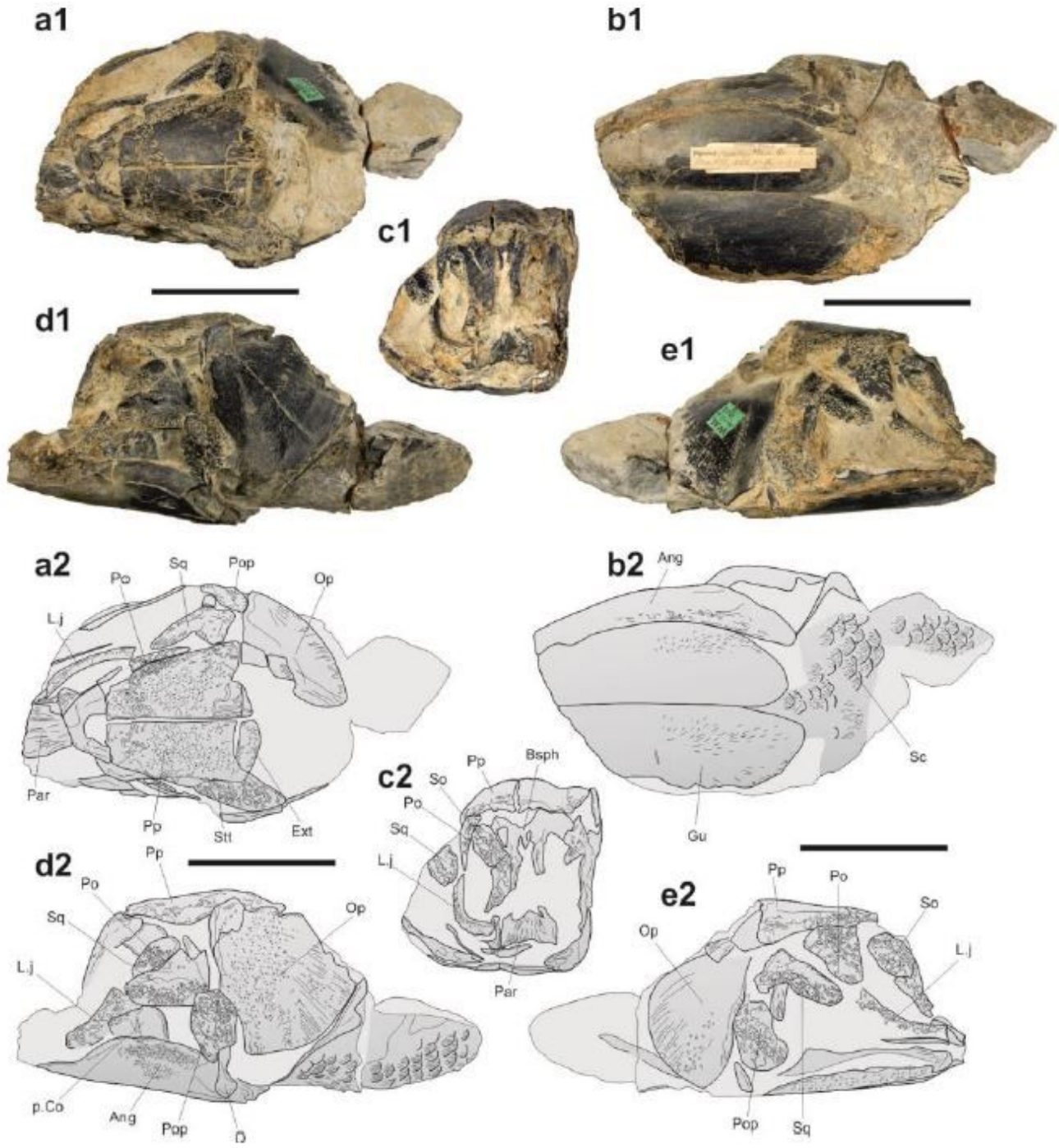

Figure 4

Trachymetopon (“Macropoma”) substriolatum (holotype, SMC J27415) from the Kimmeridgian of Cottenham, Cambridgeshire. Photograph (1) and semi-interpretative drawings in dorsal (a), ventral (b), anterior (c), left lateral (d) and right lateral (e) views. Scale bars = 50 mm. Abbreviations: Ang, angular; Bsph, basisphenoid; Ext, extrascapular; Gu, gular; L.j, lachrymojugal; Op, opercle; Par, parasphenoid; p.Co,

principal coronoid; Pop, postparietal; Pp, postparietal; Po, postorbital; Q, quadrate; Sc, scale; So, supraorbital; Sq, squamosal; Stt, supratemporal.

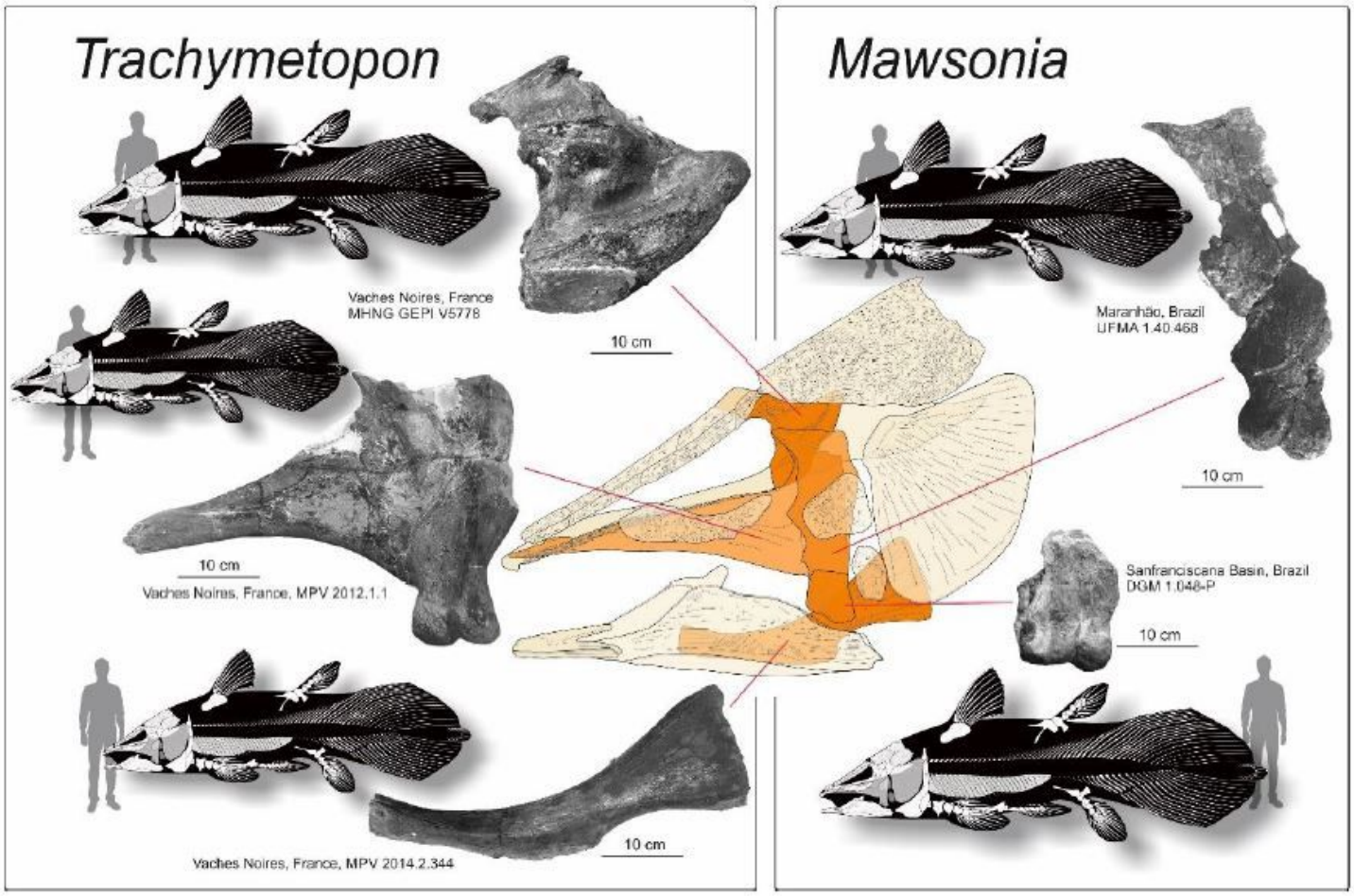

Figure 5

Fragmentary elements from the giant specimens of the Jurassic Trachymetopon and the Cretaceous Mawsonia. Human silhouettes corresponds to 1.8 m.

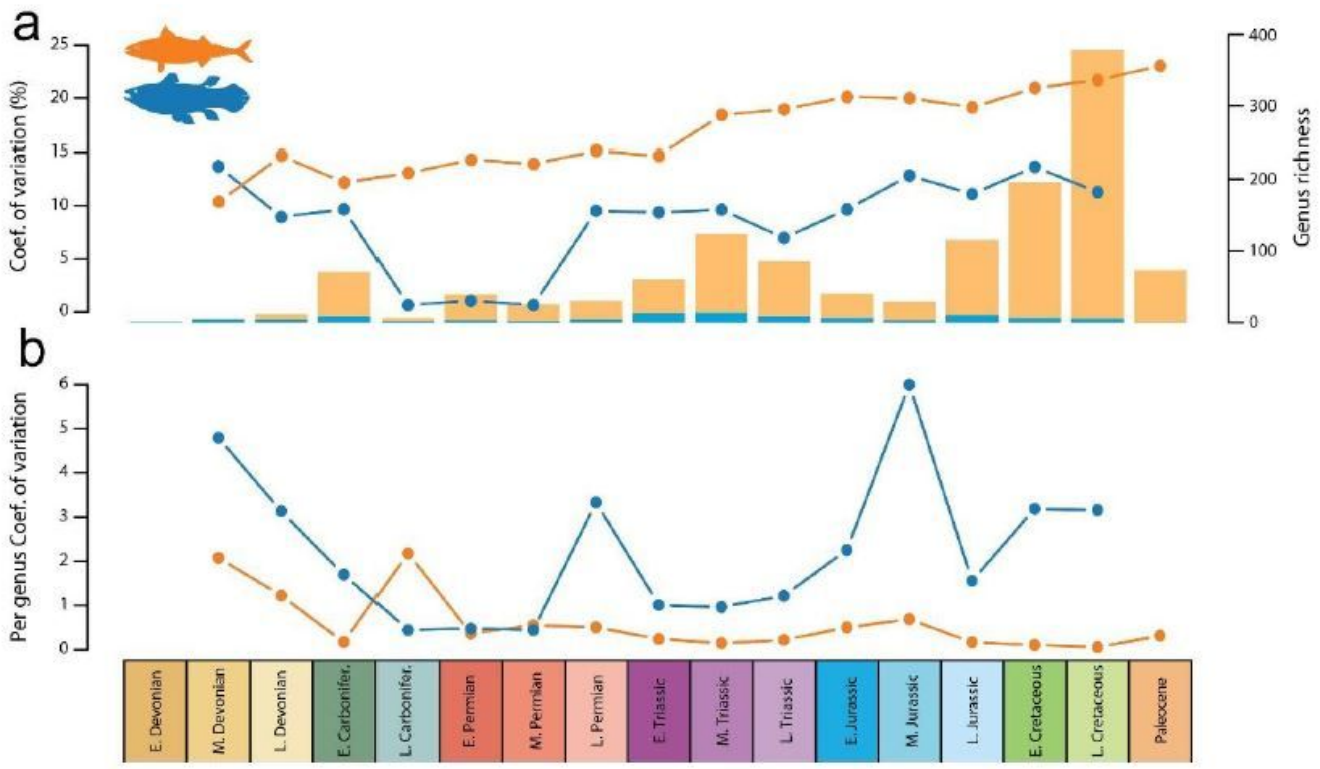

Figure 6

a, range-through genus richness (histograms) and disparity expressed by the coefficient of variation (dots and lines); b, per genus coefficient of variation, which is the coefficient of variation standardized by taxic diversity. Orange, Actinopterygii; blue, Actinistia.

Supplementary Files

This is a list of supplementary files associated with this preprint. Click to download.

- CavinetalcoelacanthsSII.pdf
- CavinetalSIbodysize.xlsx
- Media1.wmv